Proceedings of the 9ICEG
9th International Congress on Environmental Geotechnics
25-28 June, 2023 | Chania, Greece
© Authors: All rights reserved, 2023
https://doi.org/10.53243/ICEG2023-178

A case study on district-scale geothermal system potential for the city of Cambridge, UK

M. J. Kreitmair[1], N. Makasis[1], R. Ward[3] and R. Choudhary[4]

[1]*Research Associate, University of Cambridge, Cambridge, United Kingdom, email: mk2040@cam.ac.uk*

[2]*Research Associate, University of Cambridge, Cambridge, United Kingdom, email: nm735@cam.ac.uk*

[3]*Research Associate, The Alan Turing Institute, London, United Kingdom, email: rward@turing.ac.uk*

[4]*Professor, University of Cambridge, Cambridge, United Kingdom, email: rc488@cam.ac.uk*

ABSTRACT

Ground-source heat pump (GSHP) systems can be used to efficiently heat and cool buildings. However, these systems often have prohibitively high capital costs for homeowners considering small-scale installations. This work explores coordinated large-scale GSHP deployment, which can overcome this barrier to entry while also increasing the system efficiency by better utilising the ground. The city of Cambridge, UK, is adopted as a case-study site to showcase the opportunity to support decarbonisation of city thermal energy networks using district-scale GSHP systems. Finite element modelling techniques are used to simulate geothermal energy system performance and ground response, in combination with geographic information system tools incorporating local data on the natural and built environment. In addition to assessing the potential for geothermal energy utilisation, the fragmented land ownership across the study site is taken into consideration to allow identification of cost-efficient solutions and opportunities for the main stakeholders. Comparing uncoordinated and separate GSHP systems to a single neighbourhood-scale coordinated system, significant performance efficiency improvements were found, resulting in estimated cost savings of about £110,000 over a 20-year operating period. The performance increase of combining heating and cooling demand is showcased, stressing the need to identify sources of heating and cooling during planning. Moreover, combining sufficiently different thermal loads resulted in better performance compared to individual systems, even when the load profiles were in the same mode, suggesting that coordinated systems can have a wide range of applications within urban environments.

Keywords: Shallow geothermal energy; underground climate; subsurface modelling, district-scale heating; ground-source heat pump systems

1 INTRODUCTION

Decarbonization of heat is one of the critical challenges facing public and private entities globally, in terms of both cost and technical viability. The UK has committed to significantly reduce greenhouse gas emissions by 2035 and reach net zero by 2050. To achieve this, all emissions from space heating and cooling and hot water provision, accounting for 40% of the UK's energy consumption and about a third of its greenhouse gas emissions, need to be eliminated (BEIS, 2021b). Geothermal energy can be harvested using ground-source heat pump (GSHP) systems to efficiently provide heating, cooling and hot water to buildings by using the ground as a heat source or sink, thereby reducing the need for using fossil fuels for heating and lowering electricity consumption and carbon emissions (Abesser & Walker, 2022; Narsilio & Aye, 2018). These systems exchange heat with the ground using ground heat exchangers (GHEs), typically in vertical borehole configurations with pipes circulating a carrier fluid and transferring heat to/from the ground.

Research has shown that coordinated district-scale systems (as opposed to stand-alone building level systems) can help mitigate the challenges to decarbonisation by making use of economies of scale (Aditya & Narsilio, 2020; BEIS, 2021a; Mikhaylova, Choudhary, Soga, & Johnston, 2016). Utilising district-scale geothermal systems can be a more efficient way to make use of the limited ground resources, optimising the delivery of thermal energy. Combining different thermal demand profiles for

various buildings can result in limited thermal accumulation in ground over long-term system operation, limiting the degradation of system efficiencies over time. Moreover, planning for a district- (or larger community-) scale system promotes equitable and sustainable usage of the ground, even during peak demand, where stand-alone independently designed GSHP systems placed in close proximity can interfere with each other's performance. This can be particularly relevant in cases with significant groundwater flow where thermal effects can be carried further afield through convection (Meng, Vienken, Kolditz, & Shao, 2019).

This paper aims to demonstrate the benefits of coordinated efforts with respect to geothermal energy resources at neighbourhood scale. To this end, a scenario-based case study located in the city centre of Cambridge, UK, is introduced where multiple landowners with heating and cooling needs are clustered together. Two scenarios are compared: first, uncoordinated ground thermal usage, where each landowner exploits their own land through deployment of separate GSHP systems, and second, coordinated ground thermal usage, where the landowners cooperatively share heating and cooling extracted from the ground from one of the landowners only. The paper begins with and outline of the study site, in terms of its hydrogeology and the local heating and cooling demand, followed by the detailed 3D finite element model developed for the study. Comparisons between the results from the two scenarios are then discussed in terms of the thermal performance and the associated costs.

2 METHODOLOGY

2.1 Study site: central Cambridge

The work presented in this paper focusses on an area in the centre of Cambridge, shown in Figure 1a, consisting of land owned by: Downing College (boundaries shown as a blue outline), The University of Cambridge (green and red), as well as private and City Council property (grey), the latter of which is mainly included for completeness and its effect on the ground, e.g., the heat rejection from the basements. The site was chosen due to the proximity of different land-owning entities to one another, and the different demand profiles, e.g., commercial and residential, and cooling, in order to showcase the potential for the sharing of shallow geothermal energy. The heating demand that is considered in this study is that of Downing College (mixed residential and commercial) and of the Judge Business School (highlighted in green, consisting of commercial demand). Also shown in Figure 1a is the Cambridge Crystallographic Data Centre (CCDC), highlighted red, which is the main cooling demand in the modelled region.

The geological heterogeneity within the studied area is illustrated in the cross-section shown in Figure 1b with the hydraulic and thermal characteristics of the materials provided in Table 1. The geology of the site was mapped from historical borehole records for the wider Cambridge area that is maintained by the British Geological Survey (BGS). The Groundhog® Desktop Geoscientific Information System was used to develop the modelling domain, constrained by superficial deposit and bedrock geology maps, producing a 3D lithological profile for the region.

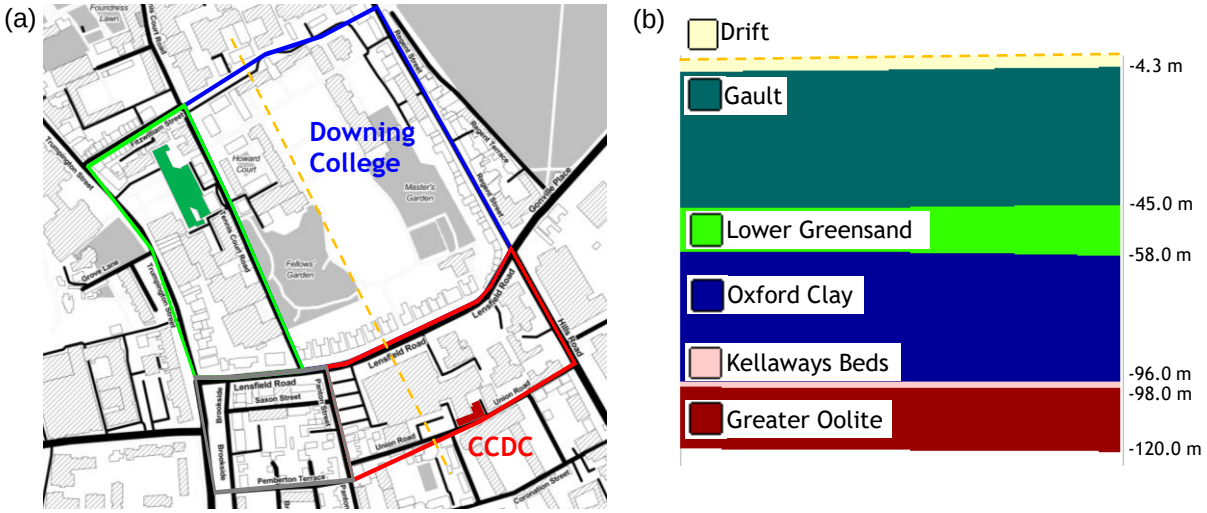


Figure 1. *Plan view of the study location with data centre highlighted in red (panel a). Geological variation at study location, along cross-section shown in the plan view as a dashed orange line (b).*

Table 1. *Thermal and hydraulic properties of the geology present in modelled domain* & GHE materials*

Material	Thermal conductivity λ [W/(m·K)]		Heat capacity C_p [J/(kg·K)]		Density ρ [kg/m³]		Hydraulic conductivity k_h [m/s]	Porosity [-]
	Sat.	Unsat.	Sat.	Unsat.	Sat.	Unsat.		
Drift	2.20	0.77	1300	700	1800	1500	2.1×10^{-7}	0.50
Gault (G)	1.43	1.11	900	590	2070	1670	8.3×10^{-12}	0.40
Lower Greensand	2.59	0.77	530	1400	1500	1200	6.1×10^{-6}	0.28
Oxford Clay (OXC)	1.57	1.11	480	1250	1900	1600	3.0×10^{-8}	0.42
Kellaways Beds (KLB)	2.50	1.80	500	1400	2510	2450	3.0×10^{-8}	0.27
Greater Oolite (GO)	2.40	1.80	900	900	2230	1980	1.7×10^{-4}	0.20
Concrete	1.80		880		2300		-	-
HDPE pipes	0.51		-		-		-	-

*(A Forster et al., 1995; Banks, Withers, Cashmore, & Dimelow, 2013; Bell, 1981; BGS, 2020, 2022; British Geological Survey (BGS), n.d.-b, n.d.-a; Busby, Kingdon, & Williams, 2011; "Densities of Sedimentary Rocks," 2017; Evans et al., 2021; Giraud, Sevostianov, Chen, & Grgic, 2015; Jones et al., 2000; Manger, 1963; Midttømme, Roaldset, & Aagaard, 1998; Revesz et al., 2019; TerraConsult Ltd, 2021; Xiong et al., 2020)

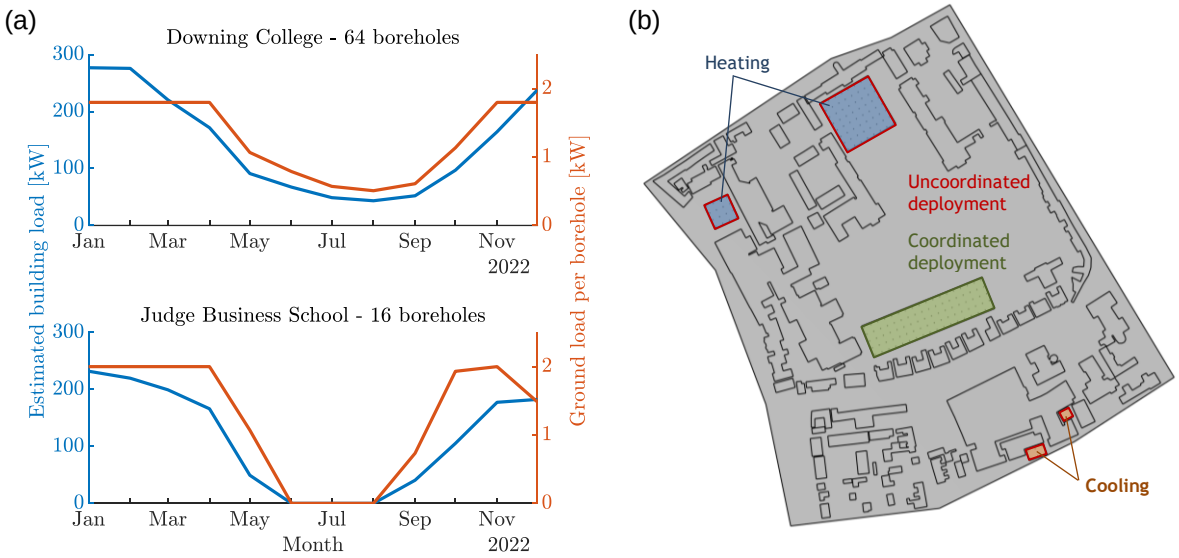


Figure 2. *Required building energy loads (left y-axis) and per borehole ground loads (right y-axis) for Downing College and the Judge Business School over one year (panel a) and borehole field configurations for uncoordinated and coordinated deployment ground thermal usage scenarios (b).*

2.2 Heating and cooling demand and borehole configurations

The estimated building heating demand for Downing College and the Judge Business School is shown in blue in Figure 2a (courtesy of University of Cambridge and Downing College Estates teams). Heating demand is highest in winter and drops to zero in summer for both sites., the ground load per borehole is shown in red, shaved at 2 kWh and 1.8 kWh for Downing College and the Judge Business School, respectively. For both buildings, a hybrid heating system is assumed, where part of the entire load is provided by the geothermal energy system, in this case about 75% for Downing College and about 25% for the Judge Business School, mainly due to space availability for the latter. Similarly for the CCDC, part of the demand is provided by the geothermal system. The cooling ground load per borehole is assumed to be a constant 2.5 kW throughout the year, supplying approximately 2 kW per borehole, towards maintaining the temperature in the server rooms of the data centre at 22 °C.

The borehole field configurations to supply heating and cooling loads for both the uncoordinated and coordinated scenarios are shown in Figure 2b. In the uncoordinated scenario, the fields outlined in red are deployed, with the two blue-shaded fields in the north of the domain, consisting of 64 (arranged in an 8-by-8 rectangular grid) and 16 (4-by-4) boreholes, supplying heating loads to Downing College and the Judge Business School (see Figure 2a) and the two orange-shaded fields in the south of the domain supplying cooling to CCDC via 10 boreholes (one 2-by-3 and one 2-by-3 field). In the coordinated scenario, only the green field is deployed, providing heating and cooling to all three buildings, consisting

of 80 heating and 10 cooling boreholes (a 5-by-18 rectangular grid), with the cooling load boreholes interspersed between the heating ones. The borehole spacing for all fields is assumed at 8 m, to minimise thermal interference and accumulation effects, and boreholes are 100 m deep.

2.3 Numerical Framework

A 3D model of the study area was created in the finite element modelling suite COMSOL Multiphysics®. Physical processes are incorporated using the conductive and convective heat transfer equations,

$$\left(\rho C_p\right)_{\text{eff}} \frac{\partial T_g}{\partial t} + \rho_f C_{p,f} \boldsymbol{v}_f \cdot \nabla T_g + \nabla \cdot \left(-\lambda_{\text{eff}} \nabla T_g\right) = 0, \quad (1)$$

where ρ_{eff} is the effective density of the ground (kg/m^3), $C_{p_{\text{eff}}}$ is the effective specific heat capacity (J/(kg·K)), T_g is the ground temperature (°C), t is time (s), ρ_f is the fluid (groundwater) density (kg/m^3), $\boldsymbol{v}_f$ is the Darcy velocity of the fluid (m/s), and λ_{eff} is the effective thermal conductivity of the ground; Darcy's law,

$$\boldsymbol{v}_f = -\frac{K}{\mu_f}\left(\nabla p_f - \rho_f \boldsymbol{g}\right), \quad (2)$$

where K, the ground permeability (m^2), and μ_f, the fluid dynamic viscosity (Pa·s), is related to the hydraulic conductivity k_h (m/s) via $K/\mu_f = k_h/(\rho_f g)$; and the continuity equation, $\nabla \cdot \left(\rho_f \boldsymbol{v}_f\right) = 0$.

The model is illustrated in Figure 3a, along with the boundary conditions applied. Hydraulically, the inflow and outflow boundaries are set to hydraulic head values of 10 and 9.5 m, respectively, based on hydrogeological measurements from the area, courtesy of the Environment Agency, and, thermally, boundary conditions to allow heat inflow and outflow are applied. Laterally to the flow, the boundaries are set to symmetry in both hydraulic and thermal physics. No-flow conditions are applied at the bottom surface and at z = -2 m, where groundwater begins. The temperature at the top surface of the model is set to vary over time, accounting for the seasonal air temperature fluctuation, using a semi-empirical function in depth and time (Baggs, 1983; Beardsmore & Cull, 2001), fitted to local conditions, i.e.,

$$T_g(z,t) = T_{0,g} - 1.07 k_v T_{\text{amp}} e^{-\epsilon z} \cos[\omega(t - t_0) + \epsilon z], \quad (3)$$

where $T_{0,g}$ is the mean annual ground temperature (°C), set to 13.1 °C based on ground investigations in the area (courtesy of University of Cambridge Estates), T_{amp} is the amplitude of the seasonal air temperature fluctuation (°C), found to be 6.8 °C, ω is the angular frequency of the heating cycle (rad) with period $P = 365$ days $\epsilon = \sqrt{\pi/(P\alpha)}$, α is the thermal diffusivity of the ground (m^2/s), k_v is the shade factor coefficient (varying between 0.3 and 1.3 depending on the conditions present (Popiel & Wojtkowiak, 2013), and using 0.8 for the chosen area), and t_0 is the day of coldest temperature after January 1st, found to be 26 days. The initial temperature throughout the soil domains is set to $T_{\text{farfield}} =$ 13.1 °C. The temperature at the bottom boundary of the domain is set to 14.9 °C, based on the findings of the previously mentioned hydrogeological investigations. Basements are set to have a temperature boundary condition of 18 °C to incorporate the expectation that the basements are heated.

The GHE operation is incorporated in detail in the model, by modelling the boreholes using 3D elements and the pipes using 1D elements, assuming a uniform pipe flow. To simulate the flow within the pipes, the governing equations for continuity and momentum for an incompressible fluid are used:

$$\nabla.(A\rho_w \boldsymbol{v_w}) = 0, \quad (4)$$

$$\rho_w \left(\frac{\partial \boldsymbol{v_w}}{\partial t}\right) = -\nabla p_w - f_D \frac{\rho_w}{2d_h} |\boldsymbol{v_w}| \boldsymbol{v_w} \quad (5)$$

where *A* is the inner cross-section of the HDPE pipe, ρ_w is the density of water, $\boldsymbol{v_w}$ represents the water velocity field in the pipes embedded within the GHEs, t is the time, p_w is the water pressure, f_D represents the Darcy friction factor, and d_h is the hydraulic diameter of the pipe. The energy equation to describe the convective–conductive heat transfer within the pipes for an incompressible fluid is:

$$\rho_w A C_{p,w} \frac{\partial T}{\partial t} + \rho_w A C_{p,w} \boldsymbol{v_w} \nabla T = \nabla(A\lambda_w \nabla T) + f_D \frac{\rho_w A}{2d_h} |\boldsymbol{v_w}| \boldsymbol{v_w}^2 + Q_{\text{wall}}, \quad (6)$$

$$Q_{\text{wall}} = f(T_{\text{pipe wall}}, T) \quad (7)$$

where $C_{p,w}$ and λ_w are the specific heat capacity and thermal conductivity of water respectively, and Q_{wall} is the external heat exchange rate through the pipe wall, expressed as a function of the temperature of the pipe outer wall, $T_{\text{pipe wall}}$, and the temperature of the water, T. The above equations are solved for the pressure p_w, the velocity field $\boldsymbol{v_w}$, and the temperature field T in the water and are

coupled to the temperature field T_g obtained from the domain heat transfer equations (Eq. 1). The fluid flow rate within the 32 mm outer diemeter GHE pipes is set to 11 L/min and the required ground load is enforced by setting the temperature of the fluid entering the GHE.

Figure 3b shows an example of the mesh used for the numerical model, with a finer mesh used to resolve smaller components in the model. For the top layers (down to 4 m) and throughout the depth for the borehole fields, detailed free tetrahydral meshes are uilised, while for the remaining ground a swept mesh is implemented to ensure reasonable computational running times on the order of 1-2 days per model for an analysis period of 20 years.

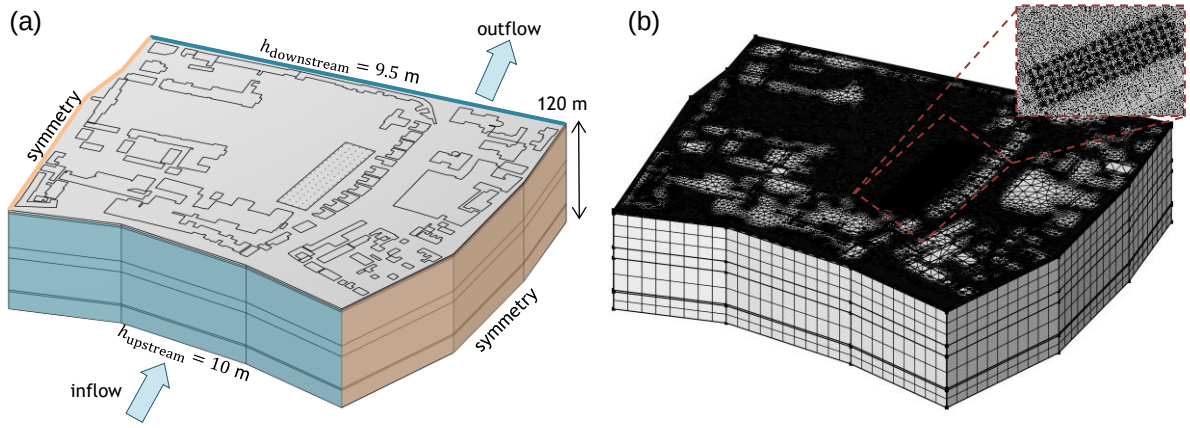


Figure 3. *Illustration of the numerical model and boundary conditions (panel a) and mesh used for the model and close up of the borehole field (b) for the coordinated scenario.*

3 RESULTS AND DISCUSSION

3.1 Temperature comparison and ground response

A comparison between the uncoordinated and coordinated borehole deployments, in terms of the resulting ground temperature is given in Figure 4. These results represent the state of the ground after 20 years of operating the GSHP systems, at 10 m below ground level. A similar relative thermal response was found throughout the depth. For the uncoordinated scenario (panel a) the three separate borehole fields operate in one mode, namely heating for Downing College (DC) and the Judge Business School (JBS) and cooling for the Cambridge Crystallographic Data Centre (CCDC). This results in a relatively uniform decrease in the temperatures within the borehole fields over time for the two heating mode fields and increase for the cooling mode field. On the other hand, in the coordinated scenario (panel b), temperatures are seen to both decrease and increase within the borehole field, notably reducing thermal accumulation. For both scenarios, the heated basement footprints can also be seen, contributing, in a localised way, to the amount of heat stored in the ground.

The average fluid temperature within GHE pipes is an indicator for the thermal performance of the system. The more extreme the temperature is (low for heating and high for cooling modes), the harder it is for the heat pump to extract or reject heat. The temperature needs to be within the heat pump operating limits, typically from -5 °C to about 40 °C, for the system to operate and to avoid potentially altering the ground thermal regime. Figure 5 shows the fluid temperatures over the 20-year period of operating the GSHP systems for each of the described scenarios. In the uncoordinated scenario (Figure 5a), the cooling system for the CCDC results in steadily increasing fluid temperatures, reaching a maximum of 31.7 °C after 20 years. In the DC and JBS GSHP systems, the temperatures decrease over time, reaching -2.6 °C and 0.3 °C, respectively, approaching the operating limits of the heat pump. In the coordinated scenario (Figure 5b), the fluid temperature of CCDC system initially increases, but after about 2 years of operation begins to decrease as the temperature of the borefield overall starts decreasing due to the thermal impact of operating the nearby boreholes in heating mode, as observed in Figure 4. The fluid temperatures in the coordinated borefields for DC and JBS reaches temperatures of just above 0 °C, showing that a combined system significantly increases the minimum temperature for DC and has only a minor impact on the JBS system, by better distributing the combined thermal load.

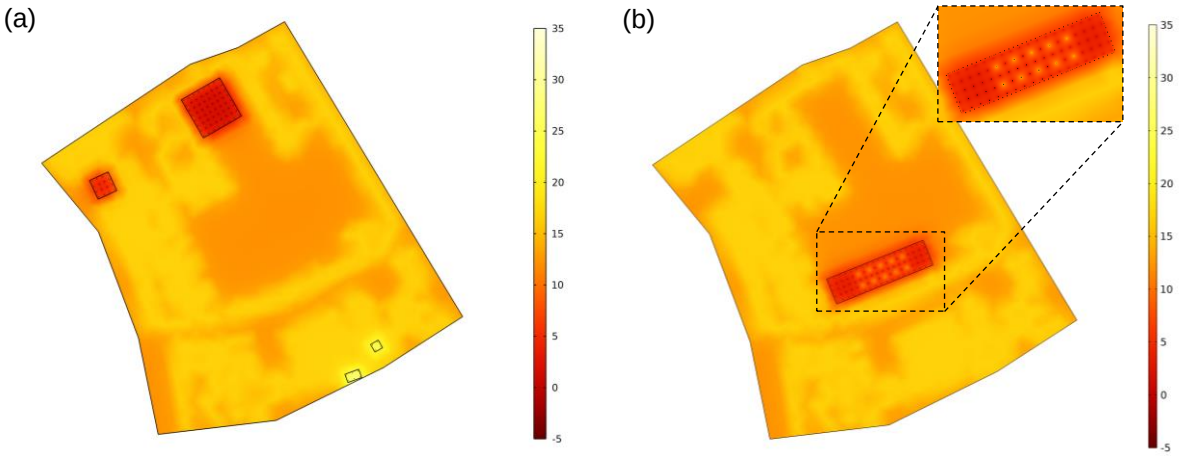


Figure 4. *Heatmaps showing the ground temperature at 10 m below ground level after 20 years of operation for the uncoordinated scenario (panel a) and the coordinated one, with inset showing close-up of the borehole field (b).*

Furthermore, considering the benefits a coordinated system can have, a third scenario was simulated where the 5 boreholes in the right-most column of the 5-by-18 configuration borefield were removed. In this scenario, the CCDC fluid temperatures reduce earlier and faster, shown in Figure 5c, as the thermal load per heating borehole is now higher. The DC and JBS fluid temperatures reach -1.32 °C, which is still higher than the DC temperatures in the uncoordinated scenario. The results suggest that, with proper coordination of operating geothermal energy systems, significant reductions in the capital costs may be achieved.

3.2 Efficiency and cost analysis

To better quantify the performance difference between the scenarios, the coefficient of performance (COP) for heating and the energy efficient ratio (EER) for cooling is calculated for each case, over the 20-year operational period. These performance ratings are computed as the ratio of supplied heating and cooling to the amount of energy consumed, thereby representing the energy efficiency of the system. In this study, these values are computed based on the fluid temperatures entering the heat pump using technical specifications of a typical geothermal heat pump (e.g., ClimateMaster™ Tranquility® 30 Digital (TE) Series Models TED/H/V 072 60Hz). A value of £0.34/kWh is assumed for the cost of electricity. Comparing the operational costs for the uncoordinated and coordinated scenarios, it is expected that the latter would incur additional pumping costs due to the distance of the buildings from the borefields, which are not included in this analysis, but are estimated at around £25,000 over 20 years for combined heating and cooling using typical values and the Darcy–Weisbach equation to calculate the pressure difference.

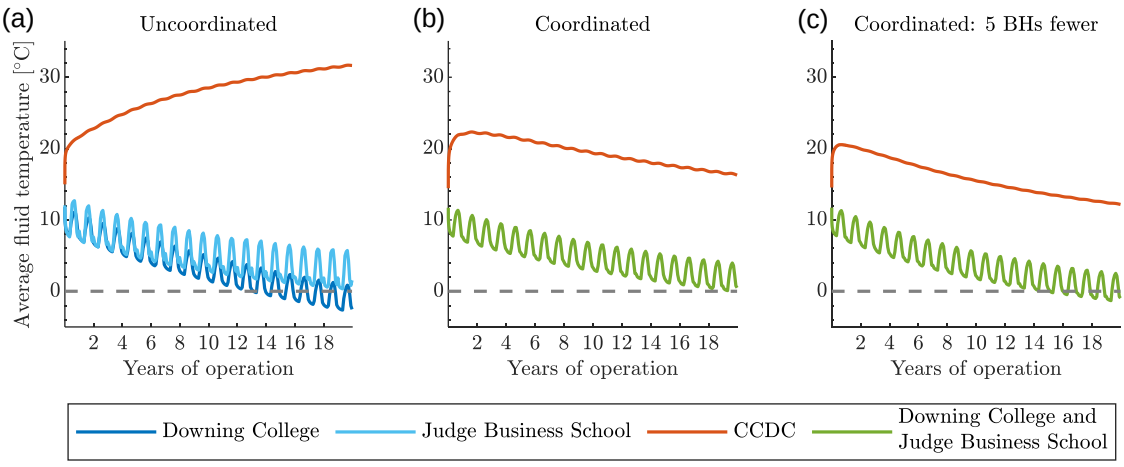


Figure 5. *Average fluid temperature in the boreholes supplying heating for Downing College and the Judge Business School and cooling to the CCDC over 20 years of operation for the uncoordinated scenario (panel a), the coordinated scenario (b), and the coordinated scenario with five fewer boreholes deployed (c).*

The results of COP and EER varying over time are shown Figure 6a. The COP values for each of the three scenarios (i.e., uncoordinated DC and JBS and coordinated DC and JBS combined), show a decrease in performance over the 20 years, as the fluid temperatures decrease and the heat pump requires more energy to extract the heat. However, the coordinated heating scenario (green in Figure 6a) decreases to a minimum COP of 3.56, compared to the uncoordinated scenario of 3.60 for JBS (light blue in Figure 6a) and 3.38 for DC. Given that 80% of the produced energy is for DC, combining the heating demands of DC and JBS can result in a better performance for the majority of the produced energy and only marginally reduced performance for the remaining 20% of the heating energy. These results are reflected in the cost estimates (Figure 6b) where the total operating costs over 20 years are reduced by £66,000 or 3%. In addition to the cost reductions, a higher COP ensures the system could operate for a longer period of time before requiring maintenance or the ground temperature is significantly impacted.

The cooling performance of the two scenarios, on the other hand, is vastly different. While in the uncoordinated scenario, the EER reduces over time, as the ground and the circulating fluid become hotter, the coordinated scenario is more sustainable because the boreholes for heating and cooling are in close proximity. This lowers the ground temperature over time, making it less costly to reject heat into the ground. The operating savings between the two scenarios are about £44,000, a reduction of 17%. Importantly, since the performance of the coordinated cooling system does not degrade over time, and in fact improves, it is not limited in its operating time and could be running efficiently for many years. In this study, an available thermal load was utilised for the CCDC, however, if a higher cooling load was required, a well-designed, site-specific coordinated system could ensure that neither COP nor EERs would significantly degrade over time. Heating rejected into the ground from the boreholes used for heating would be exchanged by the boreholes used for heating establishing thermal equilibrium. While this phenomenon is dependent on the total amount of heating and cooling required, our study showcases that cooling-dominant buildings, such as data centres (becoming increasingly necessary in the modern world), could be cooled very efficiently using geothermal energy systems, when combined with nearby heating demand.

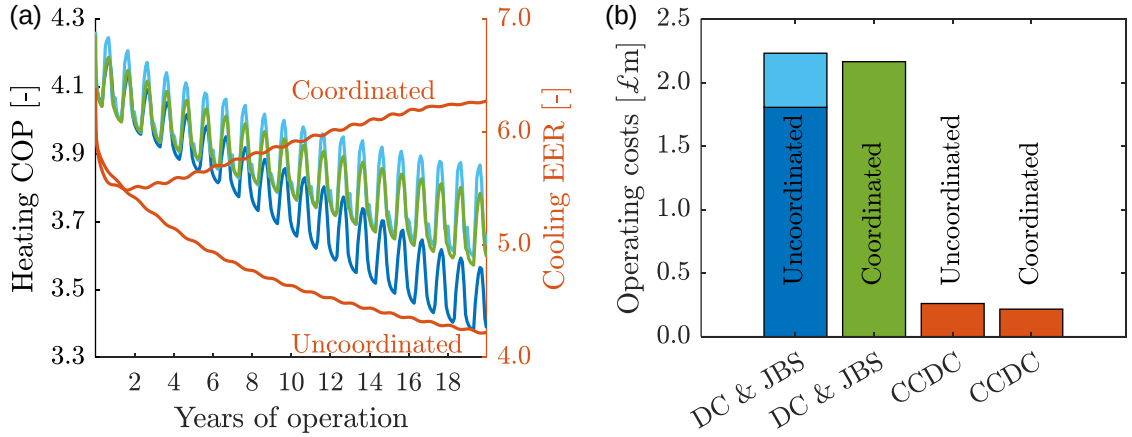


Figure 6. *Cost analysis results, showing the operational performance of heating COP for Downing College and the Judge Business School, and Cooling EER for the CCDC (panel a), and the operational costs after 20 years (b), for both uncoordinated and coordinated scenarios. Note, the colour scheme is the same as in Figure 5.*

The previous analysis investigated the operational costs only, as most sources of information on the capital costs report values per metre of borehole drilled, which is identical for the above scenarios. However, an additional third scenario was introduced, where the boreholes used for heating are reduced by five (i.e., by removing the rightmost column of the borehole field). This design decision reduces the overall capital costs required for installing the boreholes (by having fewer boreholes overall). To highlight the difference, this analysis includes capital costs and assumes a borehole installation cost value of £70 per metre depth. However, it is worth noting that in both cases, i.e., 90 or 85 total boreholes, it is likely that the coordinated system would incur significantly lower capital costs due to constructing the field in a single project, instead of three separate phases. Thus, significant cost reductions can be expected which are not accounted herein, due to equipment mobilisation costs and disruption costs (e.g., road and footpath closures, high levels of noise), among others.

The performance and cost estimates for the uncoordinated and coordinated scenarios with five fewer boreholes are shown in Figure 7. Unsurprisingly, the COP values for the coordinated case is lower when there are fewer boreholes, as each borehole exchanges more heat with the ground, with a minimum value of 3.48 (Figure 7a green line). This value is still better than the uncoordinated COP for DC (minimum 3.38 dark blue line). Over the 20-year operating period, the reductions in cost between uncoordinated and coordinated scenarios is about £50,000, which is lower than the reduction when the borehole number was the same for uncoordinated and coordinated scenarios. The EER for the coordinated cooling scenario further increases with fewer heating boreholes and reaches a maximum EER of 6.53 compared to 6.27 for the original coordinated scenario. This is because the temperature of the ground immediately next to the cooling boreholes reduces faster, due to the higher amount of heating being exchanged per borehole. This phenomenon improves the system performance and increases the cost reduction to £55,000.

When comparing the total cost reduction in costs for the uncoordinated and coordinated scenarios with both heating and cooling over an operation of 20 years, using the same number of boreholes results in a reduction of £110,000. In comparison, with fewer boreholes the cost reduction in the coordinated scenario is £105,000. The estimates are very similar and indicate that there is significant room for optimisation and savings with coordinated use of the ground, especially when addressing both heating and cooling demands. Furthermore, aspects such as land ownership and capital could also be incorporated into the cost analysis, e.g., by considering entities with significant land installing large-scale geothermal systems and distributing heating and cooling across neighbourhoods or districts for profit, thus both optimising the utilisation of the ground and system performance as well as offering efficient, sustainable heating and cooling to the general public without the high capital cost experienced by individual GSHP system owners.

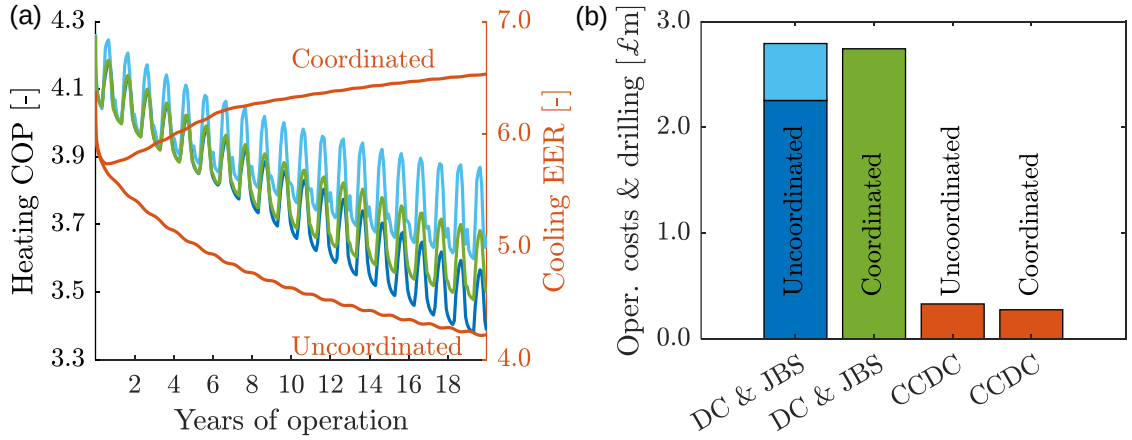


Figure 7. *Cost analysis results, showing the operational performance, Heating COP for Downing College and the Judge Business School and Cooling EER for the CCDC (panel a), and the drilling and operational costs after 20 years (b), for both uncoordinated and coordinated scenarios, when the coordinated scenario reduces the number of heating boreholes by five. Note, the colour scheme is the same as in Figure 5.*

4 CONCLUSIONS

This work has investigated the application of a small district-scale geothermal system, using an example case study in the city centre of Cambridge, UK. Two scenarios were considered, in which three distinct heating and cooling systems were designed: first, a separate or uncoordinated operation across three separate locations; and second, coordinated operation, including a dual use borefield. Heating consumption data from buildings in the area were used to estimate the heating demand and geological and hydrological field investigation data were used to accurately represent the ground conditions. The scenarios were simulated in high resolution using detailed 3D finite element modelling, for an operating period of 20 years.

The analyses have shown that coordinated usage of the ground can result in significant cost savings and a prolonged design life for geothermal energy systems. The supply of heating and cooling from within the same borefield was shown to be particularly efficient, with the rejection and extraction of heat

counteracting any thermal impacts to the ground. Specifically, the inclusion of a small number of boreholes for cooling resulted in vastly different efficiencies between the uncoordinated and coordinated scenarios, with an EER increase of 48% after 20 years, and increasing (instead of decreasing) the system performance for cooling over time. The coordinated heating system resulted in better weighted performance compared to two separate systems for the uncoordinated scenario (COP of 3.56 compared to 3.42 after 20 years), showing that combining relatively different heating profiles in one system can be beneficial. The coordinated system resulted in savings of about £110,000. In addition, a coordinated system scenario with (five) fewer boreholes was also considered, resulting in a performance similar to that of the uncoordinated scenario for heating, that significantly improved cooling performance (by about 55%), and had similar total cost savings of about £105,000.

Overall, the results in this work highlight the potential that coordinated neighbourhood- or district-scale geothermal energy systems have, to harmonise the operation, increase performance, and utilise the ground in a more sustainable and cost-effective way.

5 ACKNOWLEDGEMENTS

This work was supported by CMMI-EPSRC: Modeling and Monitoring of Urban Underground Climate Change (EP/T019425/1), by the Centre for Smart Infrastructure \& Construction (EP/N021614/1) and the Centre for Digital Build Britain at University of Cambridge, as well as AI for Science and Government (ASG), UKRI's Strategic Priorities Fund awarded to the Alan Turing Institute, UK (EP/T001569/1). The authors would like to thank the British Geological Survey, the Environment Agency, and the University of Cambridge Estates for supplying information and relevant data to enable accurate modelling of the geothermal systems in this work.

REFERENCES

A Forster, P R N Hobbs, Cripps, A. C., Entwistle, D. C., Fenwick, S. M. M., Raines, M. R., … Meakin, J. L. (1995). Engineering Geology of British Rocks and Soils: Gault Clay.

Abesser, C., & Walker, A. (2022). POSTbrief: Geothermal Energy. In Renewable Energy Technologies and Water Infrastructure. https://doi.org/10.1061/9780784415856.ch8

Aditya, G. R., & Narsilio, G. A. (2020). Environmental assessment of hybrid ground source heat pump systems. Geothermics, 87, 101868. https://doi.org/10.1016/j.geothermics.2020.101868

Baggs, S. A. (1983). Remote prediction of ground temperature in Australian soils and mapping its distribution. Solar Energy, 30(4), 351–366. https://doi.org/10.1016/0038-092X(83)90189-5

Banks, D., Withers, J. G., Cashmore, G., & Dimelow, C. (2013). An overview of the results of 61 in situ thermal response tests in the UK. Quarterly Journal of Engineering Geology and Hydrogeology, 46(3), 281–291. https://doi.org/10.1144/qjegh2013-017

Beardsmore, G. R., & Cull, J. P. (2001). Heat Generation. In Crustal Heat Flow (pp. 23–44). https://doi.org/10.1017/cbo9780511606021.003

BEIS. (2021a). Heat Network Zoning. Retrieved from https://assets.publishing.service.gov.uk/government/uploads/system/uploads/attachment_data/file/1024216/heat-network-zoning-consultation.pdf

BEIS. (2021b). Policy paper: Heat and Buildings Strategy. Retrieved from https://www.gov.uk/government/publications/heat-and-buildings-strategy

Bell, F. G. (1981). A survey of the physical properties of some carbonate rocks. Bulletin of the International Association of Engineering Geology, 24(1), 105–110. https://doi.org/10.1007/bf02595261

BGS. (2020). GeoReports: Ground Source Heat Pump - vertical closed loop. Retrieved from https://shop.bgs.ac.uk/Resources/Shop/doc/example/Product/GRC_C107.pdf

BGS. (2022). GeoReports: Temperature and Thermal Properties (Detailed). (October 2020), 1–24. Retrieved from https://shop.bgs.ac.uk/resources/shop/doc/example/product/modules/C011.pdf

British Geological Survey (BGS). (n.d.-a). Chalk aquifer properties. Retrieved February 10, 2023, from https://www2.bgs.ac.uk/groundwater/waterResources/thames/chalk.html

British Geological Survey (BGS). (n.d.-b). Lower Greensand aquifer properties. Retrieved February 10, 2023, from https://www2.bgs.ac.uk/groundwater/waterResources/thames/lowerGreensand.html

Busby, J., Kingdon, A., & Williams, J. (2011). The measured shallow temperature field in Britain. Quarterly Journal of Engineering Geology and Hydrogeology, 44(3), 373–387. https://doi.org/10.1144/1470-9236/10-049

COMSOL Multiphysics® v. 6.1. www.comsol.com. COMSOL AB, Stockholm, Sweden.

Densities of Sedimentary Rocks. (2017). Retrieved February 13, 2023, from https://gpg.geosci.xyz/content/physical_properties/tables/density_sedimentary_rocks.html

Evans, D. L., Quinton, J. N., Tye, A. M., Rodés, Rushton, J. C., Davies, J. A. C., & Mudd, S. M. (2021). How the composition of sandstone matrices affects rates of soil formation. Geoderma, 401(October 2020). https://doi.org/10.1016/j.geoderma.2021.115337

Giraud, A., Sevostianov, I., Chen, F., & Grgic, D. (2015). Effective thermal conductivity of oolitic rocks using the Maxwell homogenization method. International Journal of Rock Mechanics and Mining Sciences, 80, 379–387. https://doi.org/10.1016/j.ijrmms.2015.10.010

Jones, H. K., Morris, B. L., Cheney, C. S., Brewerton, L. J., Merrin, P. D., Lewis, M. A., … Robinson, V. K. (2000). The Physical Properties of Minor Aquifers in England and Wales. In British Geological Survey Technical Report.

Manger, G. E. (1963). Porosity and Bulk Density of Sedimentary Rocks: Contributions to Geochemistry. Geological Survey Bulletin 1144-E, 60.

Meng, B., Vienken, T., Kolditz, O., & Shao, H. (2019). Evaluating the thermal impacts and sustainability of intensive shallow geothermal utilization on a neighborhood scale : Lessons learned from a case study. Energy Conversion and Management, 199(111913). https://doi.org/10.1016/j.enconman.2019.111913

Midttømme, K., Roaldset, E., & Aagaard, P. (1998). Thermal Conductivity of Selected Claystones and Mudstones from England. Clay Minerals, 33, 131–145. https://doi.org/10.1180/claymin.1998.033.1.12

Mikhaylova, O., Choudhary, R., Soga, K., & Johnston, I. W. (2016). Benefits and optimisation of district hybrid ground source heat pump systems. Energy Geotechnics - Proceedings of the 1st International Conference on Energy Geotechnics, ICEGT 2016, 535–544. https://doi.org/10.1201/b21938-85

Narsilio, G. A., & Aye, L. (2018). Shallow Geothermal Energy: An Emerging Technology. In A. Sharma, A. Shukla, & L. Aye (Eds.), Low Carbon Energy Supply (pp. 387–411). Springer Singapore.

Popiel, C. O., & Wojtkowiak, J. (2013). Temperature distributions of ground in the urban region of Poznan City. Experimental Thermal and Fluid Science, 51, 135–148. https://doi.org/10.1016/j.expthermflusci.2013.07.009

Revesz, A., Chaer, I., Thompson, J., Mavroulidou, M., Gunn, M., & Maidment, G. (2019). Modelling of heat energy recovery potential form underground railways with nearby vertical ground heat exchangers in an urban environment. Applied Thermal Engineering, 147(October 2018), 1059–1069. https://doi.org/10.1016/j.applthermaleng.2018.10.118

TerraConsult Ltd. (2021). ELSTOW SOUTH LANDFILL SITE: HYDROGEOLOGICAL RISK ASSESSMENT.

Xiong, J., Lin, H., Ding, H., Pei, H., Rong, C., & Liao, W. (2020). Investigation on thermal property parameters characteristics of rocks and its influence factors. Natural Gas Industry B, 7(3), 298–308. https://doi.org/10.1016/j.ngib.2020.04.001